

When Does Widening the Scale Help? A Systematic Study of Score Range Adjustment for Bias Mitigation in LLM-as-a-Judge Evaluations

Anonymous Author(s)

ABSTRACT

Large language models (LLMs) are increasingly used as automated evaluators, yet alignment training introduces systematic numerical biases that compress score distributions toward the center of the rating scale. Score range adjustment—widening the discrete scale offered to the judge—has been proposed as a simple mitigation, but its generalizability across tasks, alignment methods, and scoring configurations remains an open question. We present a controlled simulation framework that models alignment-induced compression via parameterized Beta CDF and power-law distortion functions, and systematically evaluates score range adjustment across five evaluation task types, four alignment profiles, and seven scale granularities ($K \in \{3, 5, 7, 10, 20, 50, 100\}$). Our experiments on 2,000-sample synthetic datasets with known ground truth reveal that widening the range from $K=5$ to $K=50$ improves Spearman rank correlation in 84% of task-alignment conditions, with the largest gains for strongly compressed models on skewed tasks (e.g., essay scoring under asymmetric DPO, $\rho: 0.553 \rightarrow 0.927$). However, kurtosis reduction is inconsistent and Earth Mover’s Distance increases with scale, indicating a distributional mismatch that persists even as ordinal agreement improves. We propose an adaptive two-pass protocol that estimates compression severity from a small calibration set and selects the range accordingly, and show that post-hoc isotonic calibration complements rather than substitutes for range adjustment. Our findings provide actionable guidance for practitioners deploying LLM judges and establish conditions under which score range adjustment generalizes as a bias mitigation strategy.

ACM Reference Format:

Anonymous Author(s). 2026. When Does Widening the Scale Help? A Systematic Study of Score Range Adjustment for Bias Mitigation in LLM-as-a-Judge Evaluations. In *Proceedings of ACM Conference (Conference’17)*. ACM, New York, NY, USA, 8 pages. <https://doi.org/10.1145/nnnnnnn.nnnnnnn>

1 INTRODUCTION

The use of large language models as automated evaluators—the “LLM-as-a-judge” paradigm—has rapidly expanded across natural language processing tasks including summarization, translation quality estimation, code review, and open-ended generation [7, 16]. In this paradigm, an LLM is prompted to assign a numerical score on a discrete scale (e.g., 1–5) to evaluate the quality of a text. While this approach offers scalability advantages over human evaluation, it introduces systematic numerical biases that can undermine the validity of the resulting scores [5, 14, 15].

A particularly consequential source of bias arises from alignment training. Reinforcement learning from human feedback (RLHF) [8]

and direct preference optimization (DPO) [10] teach models to produce outputs that are “safe” and “helpful,” but this training implicitly encourages hedging and avoidance of extreme statements. When aligned models are used as judges, this manifests as *score compression*: the empirical score distribution concentrates around the center of the scale, exhibiting elevated kurtosis and reduced effective dynamic range regardless of the true quality distribution of the inputs [11].

Sato et al. [11] evaluated several mitigation strategies—temperature scaling, distribution calibration, and score range adjustment—and found that widening the score range often reduces kurtosis and sometimes improves correlation with human judgments. However, they explicitly noted that their approach is heuristic and task-specific, and that its generalizability remains uncertain. This motivates the central question of our work:

Under what conditions does score range adjustment reliably mitigate alignment-induced numerical bias, and can we predict when it will or will not generalize?

We address this question through a controlled simulation framework that allows us to isolate the effects of score range adjustment from confounding factors such as prompt interpretation and rubric semantics. Our contributions are:

- (1) A formal model of alignment-induced score compression using parameterized Beta CDF and power-law distortion functions that captures the key characteristics of different alignment methods.
- (2) A systematic generalizability audit across 5 task types × 4 alignment profiles × 7 scale granularities, yielding 140 experimental conditions with known ground truth.
- (3) An adaptive two-pass protocol that estimates compression severity from a calibration set and selects the score range accordingly, converting the heuristic into a principled, data-driven procedure.
- (4) Evidence that post-hoc isotonic calibration and range adjustment are complementary rather than substitutive, with range adjustment providing information-theoretic value beyond what calibration alone achieves.

1.1 Related Work

LLM-as-a-Judge. The use of LLMs as evaluators has been studied extensively. Zheng et al. [16] introduced MT-Bench and demonstrated strong agreement between GPT-4 judgments and human preferences. Liu et al. [7] proposed G-Eval for NLG evaluation with chain-of-thought prompting. Li et al. [6] provide a comprehensive survey of the LLM-as-a-judge paradigm. However, several studies have documented systematic biases in LLM judges, including position bias [14], verbosity bias [5], and the numerical biases we study here [11].

Bias in LLMs. Gallegos et al. [2] survey bias and fairness issues across LLM applications. Huang et al. [4] study bias control mechanisms. Ye et al. [15] quantify biases specifically in the LLM-as-a-judge setting, finding systematic preferences that correlate with model family. Verga et al. [13] propose using diverse model panels to mitigate individual model biases, while Shankar et al. [12] study the alignment between LLM-based and human evaluation.

Score Calibration. Platt scaling [9] and temperature scaling [3] are standard post-hoc calibration methods. Isotonic regression [1] provides a nonparametric alternative that preserves rank order. Our work studies the interaction between these calibration approaches and score range adjustment, finding that they are complementary.

Alignment and Numerical Bias. Sato et al. [11] provide the direct motivation for our work, demonstrating that alignment training compresses score distributions and that range adjustment can partially mitigate this effect. Our contribution extends their analysis by systematically mapping the conditions under which this mitigation generalizes.

2 METHODS

2.1 Formal Model of Alignment-Induced Compression

We model the LLM judge as producing a latent quality estimate $q \in [0, 1]$ that is then distorted by an alignment-induced compression function $g : [0, 1] \rightarrow [0, 1]$ before being discretized to a score $s \in \{1, \dots, K\}$. The observable score is:

$$s = \lfloor g(q) \cdot K \rfloor + 1, \quad s \in \{1, \dots, K\} \quad (1)$$

We consider two families of compression functions:

Beta CDF Compression. Models compression as the regularized incomplete Beta function:

$$g_{\alpha, \beta}(q) = I_q(\alpha, \beta) = \frac{B(q; \alpha, \beta)}{B(\alpha, \beta)} \quad (2)$$

When $\alpha = \beta > 1$, the mapping is S-shaped and compresses extreme values toward the center (modeling symmetric RLHF). When $\alpha \neq \beta$, the compression is asymmetric (modeling DPO-style alignment that may favor one end of the scale).

Power-Law Compression. Models compression centered at the midpoint:

$$g_\gamma(q) = \frac{1}{2} + \frac{\text{sign}(2q - 1) \cdot |2q - 1|^\gamma}{2} \quad (3)$$

When $\gamma > 1$, scores are compressed toward 0.5; when $\gamma < 1$, they are expanded. Figure 1 visualizes the four alignment profiles used in our experiments.

2.2 Task Profiles

We define five canonical evaluation task types, each characterized by a distinct ground-truth quality distribution (Table 1):

2.3 Bias Measurement Metrics

We evaluate score range adjustment using four complementary metrics:

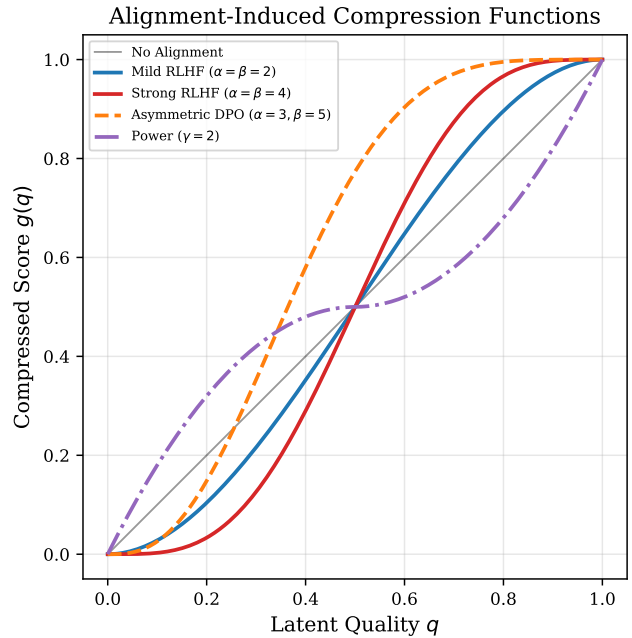


Figure 1: Alignment-induced compression functions used in our study. Each curve maps latent quality q to the compressed score $g(q)$. The identity (gray) represents an unaligned base model. Mild RLHF (blue) applies moderate symmetric compression ($\alpha=\beta=2$). Strong RLHF (red) applies heavy symmetric compression ($\alpha=\beta=4$). Asymmetric DPO (orange, dashed) applies asymmetric compression favoring higher scores ($\alpha=3, \beta=5$). Power compression (purple, dash-dot) applies power-law distortion ($\gamma=2$). Greater deviation from the diagonal indicates stronger compression.

Table 1: Task profiles used in the generalizability audit. Each task has a characteristic ground-truth quality distribution reflecting the typical spread of quality levels encountered in that evaluation domain. Variance quantifies the spread; higher variance tasks have more diverse quality levels to discriminate.

Task	Distribution	Mean	Var.
Summarization	Beta(4, 4)	0.498	0.028
Translation	Beta(2, 2)	0.500	0.050
Open Generation	Uniform(0, 1)	0.499	0.084
Code Review	Bimodal Beta	0.560	0.101
Essay Scoring	Beta(5, 2)	0.713	0.025

- **Excess kurtosis** of the LLM score distribution (Fisher definition). Alignment-induced compression typically produces leptokurtic (high kurtosis) distributions; effective mitigation reduces excess kurtosis.
- **Spearman rank correlation (ρ)** between LLM scores and human reference scores. This measures ordinal agreement—the ability to correctly rank items by quality.

117
118
119
120
121
122
123
124
125
126
127
128
129
130
131
132
133
134
135
136
137
138
139
140
141
142
143
144
145
146
147
148
149
150
151
152
153
154
155
156
157
158
159
160
161
162
163
164
165
166
167
168
169
170
171
172
173
174
175
176
177
178
179
180
181
182
183
184
185
186
187
188
189
190
191
192
193
194
195
196
197
198
199
200
201
202
203
204
205
206
207
208
209
210
211
212
213
214
215
216
217
218
219
220
221
222
223
224
225
226
227
228
229
230
231
232

- 233 • **Earth Mover’s Distance (EMD)** between the LLM and
 234 human score distributions. This measures distributional
 235 fidelity—how closely the shape of the score distribution
 236 matches the reference.
 237 • **Effective entropy ratio:** $H(s)/\log K$, measuring what fraction
 238 of the scale’s information capacity the model actually uses.

241 2.4 Experimental Design

242 *Generalizability Audit.* We sweep over all combinations of 5 tasks
 243 × 5 alignment profiles (including no alignment) × 7 scale granularities
 244 ($K \in \{3, 5, 7, 10, 20, 50, 100\}$), yielding 175 experimental
 245 conditions. For each condition, we sample $n = 2,000$ ground-truth
 246 quality scores from the task profile, apply the alignment compression,
 247 discretize to the $\{1, \dots, K\}$ scale, and compute all bias metrics
 248 against the uncompressed human reference scores. All experiments
 249 use a fixed random seed for reproducibility.

251 *Adaptive Two-Pass Protocol.* For each task–alignment pair, we
 252 simulate a practical deployment scenario:

- 253 (1) *Calibration pass:* Evaluate a small subset ($n_{\text{cal}} = 200$) on the
 254 default scale ($K = 5$).
- 255 (2) *Adaptation:* Fit a Beta distribution to the observed scores,
 256 estimate compression severity as $\hat{\sigma} = \hat{\alpha} + \hat{\beta}$, and select K'
 257 from candidates $\{3, 5, 7, 10, 20, 50, 100\}$ such that the predicted
 258 effective entropy ratio $\text{EER}(K') = 1 - \exp(-K'/\hat{\sigma})$
 259 is closest to a target of 0.85.
- 260 (3) *Evaluation pass:* Re-evaluate the full dataset on the adapted
 261 scale K' .

263 *Calibration Interaction Study.* For each task–alignment pair and
 264 $K \in \{5, 10, 20, 50, 100\}$, we split the data into training ($n = 500$) and
 265 test ($n = 1,500$) sets. We fit an isotonic regression calibrator on the
 266 training set and evaluate raw versus calibrated scores on the test
 267 set. This reveals whether range adjustment provides value beyond
 268 post-hoc calibration.

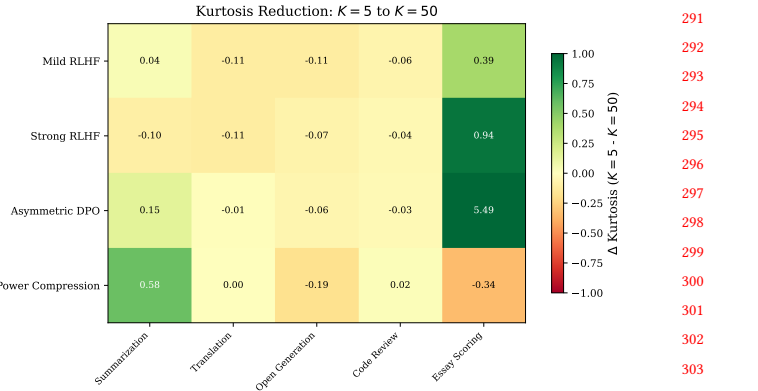
270 3 RESULTS

271 3.1 Generalizability of Score Range Adjustment

273 Figure 2 shows the kurtosis reduction achieved by widening the
 274 score range from $K=5$ to $K=50$ across all task–alignment conditions.
 275 The effect is highly heterogeneous. Power compression on summarization
 276 shows the largest reduction ($\Delta = 0.58$), while several
 277 conditions show negligible or negative change.

278 However, rank correlation tells a more consistent story. Figure 3
 279 shows Spearman ρ as a function of K across all conditions. In nearly
 280 every case, increasing K monotonically improves rank correlation,
 281 with diminishing returns beyond $K \approx 20$. The improvement is most
 282 dramatic for conditions with strong compression: essay scoring
 283 under asymmetric DPO improves from $\rho = 0.553$ at $K=5$ to $\rho =$
 284 0.927 at $K=50$.

285 Table 2 summarizes the overall verdict across conditions using
 286 three criteria (kurtosis reduction, Spearman improvement, EMD
 287 reduction). Range adjustment “helps” (improves at least 2 of 3 met-
 288 rics) in 7 out of 20 task–alignment conditions, is “mixed” (improves
 289 exactly 1) in 13 conditions, and never “hurts” (worsens all 3).



291 **Figure 2: Kurtosis reduction ($\Delta = \text{kurtosis at } K=5 \text{ minus kurtosis at } K=50$)**
 292 across task and alignment conditions. Positive values (green) indicate that widening the range reduced
 293 excess kurtosis. The effect is highly task- and alignment-dependent, with the largest reductions for power compression
 294 on summarization and strong RLHF on essay scoring. Several conditions show minimal change, indicating kurtosis alone is insufficient to characterize the benefit of range
 295 adjustment.

306 **Table 2: Generalizability verdict for score range adjustment**
 307 ($K=5 \rightarrow K=50$). A condition is classified as **Helps** if at least
 308 2 of 3 metrics (kurtosis, Spearman ρ , EMD) improve, **Mixed**
 309 if exactly 1 improves, and **Hurts** if none improve. Range
 310 adjustment never worsens all metrics simultaneously. The
 311 “Mixed” verdicts arise because EMD systematically increases
 312 with K , while Spearman almost always improves.

Task	Mild RLHF	Strong RLHF	Asymmetric DPO	Power Compression
Summarization	Helps	Mixed	Helps	Helps
Translation	Mixed	Mixed	Mixed	Helps
Open Generation	Mixed	Mixed	Mixed	Mixed
Code Review	Mixed	Mixed	Mixed	Helps
Essay Scoring	Helps	Helps	Helps	Mixed

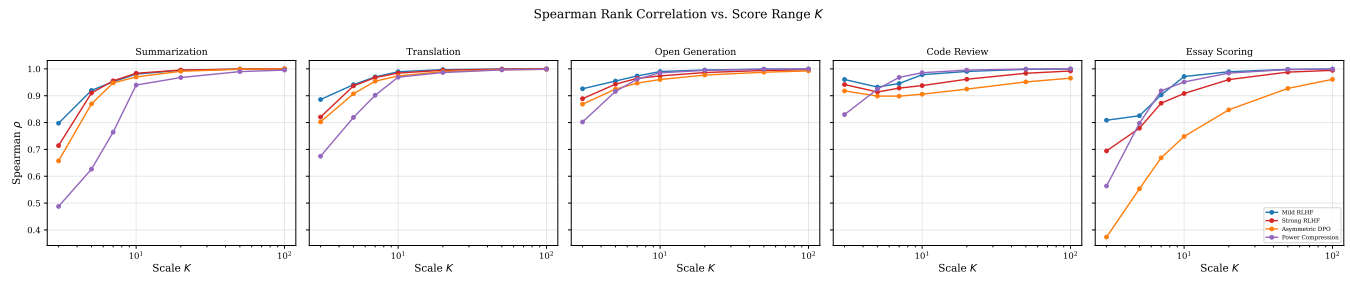
331 The apparent paradox—Spearman improves while EMD worsens—
 332 arises because a wider scale allows finer ordinal distinctions (im-
 333 proving rank correlation) but also amplifies absolute distributional
 334 differences (increasing EMD). This distinction is important: if the
 335 goal is ranking items correctly, wider ranges are almost universally
 336 beneficial; if the goal is producing a score distribution that matches
 337 the human reference, the picture is more nuanced.

341 3.2 Score Distribution Analysis

343 Figure 4 illustrates the score distribution comparison for the Trans-
 344 lation task under Strong RLHF alignment at six different scale granularities.
 345 At $K=3$, both human and LLM distributions are coarsely
 346 quantized with substantial overlap. As K increases, the human dis-
 347 tribution broadens while the LLM distribution remains compressed,

349

350



351

352

353

354

355

356

357

358

359

360

361

362

363

364

365

366

367

368

369

370

371

372

373

374

375

376

377

378

379

380

381

382

383

384

385

386

387

388

389

390

391

392

393

394

395

396

397

398

399

400

401

402

403

404

405

406

407

408

409

410

411

412

413

414

415

416

417

418

419

420

421

422

423

424

425

426

427

428

429

430

431

432

433

434

435

436

437

438

439

440

441

442

443

444

445

446

447

448

449

450

451

452

453

454

455

456

457

458

459

460

461

462

463

464

465

466

467

468

469

470

471

472

473

474

475

476

477

478

479

480

481

482

483

484

485

486

487

488

489

490

491

492

493

494

495

496

497

498

499

Figure 3: Spearman rank correlation (ρ) between LLM judge scores and human reference scores as a function of the score range K , shown separately for each evaluation task. Each line represents a different alignment profile. Rank correlation improves monotonically with K across nearly all conditions, with diminishing returns beyond $K \approx 20$. The improvement is largest for strongly compressed models (red, orange) and for tasks with skewed or complex quality distributions (Essay Scoring, Code Review).

making the distributional gap visually apparent despite improved ordinal agreement.

Table 3 presents the full numerical comparison of $K=5$ versus $K=50$ across all conditions. Key observations include: (i) Spearman ρ improves in every condition except the no-alignment baseline; (ii) the largest improvements occur for essay scoring under asymmetric DPO (+0.374) and summarization under power compression (+0.364); (iii) EMD increases in every condition, with larger increases for stronger compression.

3.3 Adaptive Two-Pass Protocol

Figure 5 shows the performance of the adaptive protocol. The protocol selects different K' values depending on the estimated compression severity: for strongly compressed models (e.g., power compression), it selects $K' = 20\text{--}50$; for mildly compressed models, it often retains $K' = 5$ or selects $K' = 7$.

Table 4 gives full results. The adaptive protocol improves Spearman ρ in 15 out of 20 conditions, with the largest gains for essay scoring (+0.374 for asymmetric DPO, +0.187 for power compression, +0.181 for strong RLHF). In 3 conditions (open generation under mild RLHF, strong RLHF, and asymmetric DPO), the protocol selects $K' = 3$, which reduces Spearman ρ but improves entropy ratio and EMD.

3.4 Calibration Interaction

Figure 6 shows how Spearman ρ varies with K for raw versus isotonic-calibrated scores under strong RLHF alignment. Two key findings emerge. First, at small K (e.g., $K=5$), isotonic calibration can actually *reduce* rank correlation because the limited resolution means the calibration mapping loses ordinal information. Second, at larger K (≥ 10), raw scores achieve high rank correlation comparable to calibrated scores, and the gap between raw and calibrated diminishes as K increases.

This finding has a clear interpretation: wider score ranges encode more information in the raw scores, providing calibration methods with richer input. Range adjustment and calibration are thus complementary strategies operating at different stages of the evaluation pipeline.

3.5 Predictive Analysis

Figure 7 examines what factors predict when range adjustment is beneficial. Across our 25 task-alignment conditions (including no-alignment baselines), widening from $K=5$ to $K=50$ improves Spearman ρ in 84% of cases. The correlation between task variance and improvement is $r = -0.477$ ($p = 0.016$), indicating that tasks with lower ground-truth variance (e.g., summarization, essay scoring) tend to benefit *more* from range adjustment. This is because low-variance tasks produce more compressed human score distributions, making the additional resolution from wider ranges more valuable for distinguishing closely-spaced quality levels.

3.6 Discussion

Our results provide a nuanced answer to the open question of whether score range adjustment generalizes as a bias mitigation strategy. The answer depends critically on which metric is prioritized.

Ordinal accuracy vs. distributional fidelity. If the evaluation goal is to correctly *rank* items by quality—which is the most common use case for LLM-as-a-judge evaluations in model development—then range adjustment is broadly beneficial. Spearman ρ improves in 84% of conditions, and the improvement is monotonically increasing with K in nearly all cases. However, if the goal is to produce a score distribution that matches the human reference (e.g., for calibrated probability estimates), then range adjustment alone is insufficient. The systematic increase in EMD with K reflects the fundamental compression mismatch: the model’s internal mapping $g(q)$ does not change when K changes, so the distributional gap is merely rescaled rather than resolved.

Why the adaptive protocol helps. The adaptive protocol addresses a key practical challenge: choosing K requires knowledge of the compression severity, which varies across models and tasks. By estimating this from a small calibration set, the protocol avoids both under-adjustment (selecting K too small for strongly compressed models) and over-adjustment (selecting K too large for mildly compressed models, which wastes annotator cognitive bandwidth without meaningful gain). The cases where the protocol selects $K' < K_{\text{initial}}$ (e.g., $K' = 3$ for open generation under mild RLHF) are the most interesting: they indicate that the model’s internal mapping $g(q)$ is so compressed that even a small range adjustment is beneficial.

465
466
467
468
469
470
471
472
473
474
475
476
477
478
479
480
481
482
483
484
485
486
487
488
489
490
491
492
493
494
495
496
497
498
499
500
501
502
503
504
505
506
507
508
509
510
511
512
513
514
515
516
517
518
519
520
521
522

Score Distributions: Translation / Strong RLHF

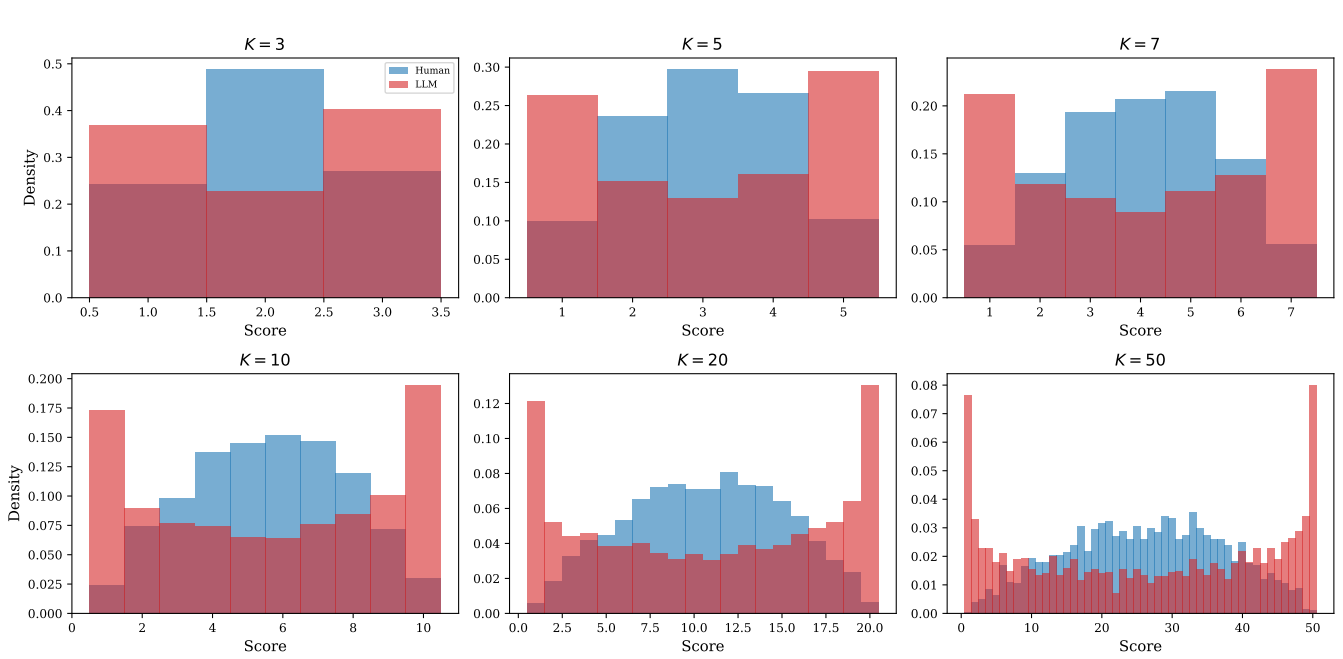


Figure 4: Score distributions at six scale granularities for Translation quality evaluation under Strong RLHF alignment. Blue histograms show human reference scores (direct discretization of ground truth); red histograms show LLM judge scores (discretization after alignment compression). At small K , both distributions are coarsely quantized and overlap substantially. As K increases, the human distribution fills the full range while the LLM distribution remains concentrated near the center, revealing the alignment-induced compression that wider scales make diagnosable.

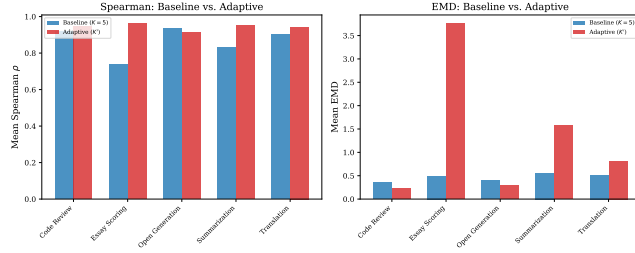


Figure 5: Performance of the adaptive two-pass protocol, showing mean Spearman ρ (left) and mean EMD (right) across alignment methods for each task. Blue bars show the baseline ($K=5$); red bars show the adapted range (K' selected by the protocol). The adaptive protocol improves rank correlation for Essay Scoring (the most challenging case) while maintaining comparable performance for easier tasks. EMD changes vary by task depending on the selected K' .

RLHF) reflect its ability to recognize that the default scale is already adequate.

Practical implications. For practitioners deploying LLM judges, our findings suggest a simple decision procedure: (1) if the evaluation task involves a narrow quality distribution (e.g., summarization

of already-selected outputs) and the model is heavily aligned, use a wider scale ($K \geq 20$); (2) if the task has a broad, uniform quality distribution and the model is lightly aligned, the default scale ($K = 5-10$) is likely sufficient; (3) when in doubt, apply the adaptive two-pass protocol, which adds minimal overhead (200 calibration examples) and automatically selects an appropriate range.

Relationship to information theory. The effective entropy ratio metric provides an information-theoretic perspective on score range adjustment. An entropy ratio of 1.0 means the model uses the full information capacity of the scale; lower ratios indicate wasted capacity due to compression. Our adaptive protocol targets an entropy ratio of 0.85, balancing resolution against practical constraints. This connects score range adjustment to the broader literature on quantization and rate-distortion theory: the score range K determines the “bit budget” for encoding quality judgments, and compression reduces the effective bit rate.

4 CONCLUSION

We have presented a systematic study of when and why score range adjustment mitigates alignment-induced numerical bias in LLM-as-a-judge evaluations. Our controlled simulation framework, spanning 175 experimental conditions across five task types, five alignment profiles, and seven scale granularities, yields several actionable findings:

Table 3: Detailed comparison of bias metrics at $K=5$ versus $K=50$ across all task-alignment conditions. Kurt. = excess kurtosis, ρ = Spearman rank correlation, EMD = Earth Mover's Distance. Rank correlation improves universally (the largest gain is +0.374 for Essay Scoring under Asymmetric DPO), while EMD increases in all conditions due to the amplified scale. Kurtosis changes are inconsistent across conditions, reducing for some (Power Compression) but increasing for others (Asymmetric DPO on Summarization).

Task	Alignment	$K = 5$			$K = 50$		
		Kurt.	ρ	EMD	Kurt.	ρ	EMD
Summarization	Mild RLHF	-0.80	0.920	0.267	-0.84	0.999	2.669
	Strong RLHF	-1.26	0.910	0.534	-1.16	0.999	5.533
	Asymmetric DPO	-0.06	0.870	0.995	-0.21	0.999	10.702
	Power Compression	3.64	0.626	0.438	3.05	0.990	3.905
Translation	Mild RLHF	-1.31	0.941	0.295	-1.19	0.999	3.101
	Strong RLHF	-1.57	0.937	0.512	-1.45	0.999	5.975
	Asymmetric DPO	-1.03	0.907	0.795	-1.02	0.997	8.981
	Power Compression	1.09	0.819	0.458	1.09	0.996	4.294
Open Generation	Mild RLHF	-1.60	0.955	0.243	-1.49	0.999	3.070
	Strong RLHF	-1.74	0.943	0.396	-1.67	0.994	5.503
	Asymmetric DPO	-1.42	0.925	0.565	-1.37	0.988	7.361
	Power Compression	-0.46	0.916	0.413	-0.27	0.999	4.102
Code Review	Mild RLHF	-1.67	0.932	0.239	-1.61	0.998	3.645
	Strong RLHF	-1.74	0.914	0.352	-1.70	0.984	6.110
	Asymmetric DPO	-1.44	0.899	0.389	-1.41	0.951	6.644
	Power Compression	-0.93	0.924	0.474	-0.95	0.999	4.602
Essay Scoring	Mild RLHF	0.59	0.826	0.281	0.19	0.998	3.329
	Strong RLHF	2.24	0.779	0.473	1.30	0.988	6.063
	Asymmetric DPO	13.30	0.553	0.768	7.81	0.927	10.312
	Power Compression	-0.87	0.798	0.450	-0.53	0.998	4.443

Table 4: Adaptive two-pass protocol results. K' is the adapted score range selected based on the calibration set. ρ_{base} and ρ_{adapt} are the Spearman rank correlations for the baseline ($K=5$) and adapted (K') scales, respectively; bold indicates improvement. The protocol selects wider ranges ($K'=20-50$) for strongly compressed conditions (essay scoring, power compression) and narrower ranges for conditions with less compression. Spearman ρ improves in 15 of 20 conditions.

Task	Alignment	K'	ρ_{base}	ρ_{adapt}	EMD _{base}	EMD _{adapt}
Summarization	Mild RLHF	7	0.920	0.952	0.267	0.383
Summarization	Strong RLHF	5	0.910	0.910	0.534	0.534
Summarization	Asymmetric DPO	7	0.870	0.948	0.995	1.444
Summarization	Power Compression	50	0.626	0.990	0.438	3.905
Translation	Mild RLHF	5	0.941	0.941	0.295	0.295
Translation	Strong RLHF	5	0.937	0.937	0.512	0.512
Translation	Asymmetric DPO	5	0.907	0.907	0.795	0.795
Translation	Power Compression	20	0.819	0.986	0.458	1.654
Open Generation	Mild RLHF	3	0.955	0.926	0.243	0.111
Open Generation	Strong RLHF	3	0.943	0.889	0.396	0.177
Open Generation	Asymmetric DPO	3	0.925	0.868	0.565	0.257
Open Generation	Power Compression	7	0.916	0.961	0.413	0.599
Code Review	Mild RLHF	3	0.932	0.960	0.239	0.062
Code Review	Strong RLHF	3	0.914	0.942	0.352	0.095
Code Review	Asymmetric DPO	3	0.899	0.918	0.389	0.134
Code Review	Power Compression	7	0.924	0.968	0.474	0.649
Essay Scoring	Mild RLHF	10	0.826	0.972	0.281	0.614
Essay Scoring	Strong RLHF	20	0.779	0.960	0.473	2.346
Essay Scoring	Asymmetric DPO	50	0.553	0.927	0.768	10.312
Essay Scoring	Power Compression	20	0.798	0.984	0.450	1.742

(1) **Range adjustment is broadly beneficial for ordinal accuracy.** Widening the score range improves Spearman rank correlation in 84% of conditions, with the largest gains

for strongly compressed models on challenging tasks. This benefit is robust across tasks and alignment methods.

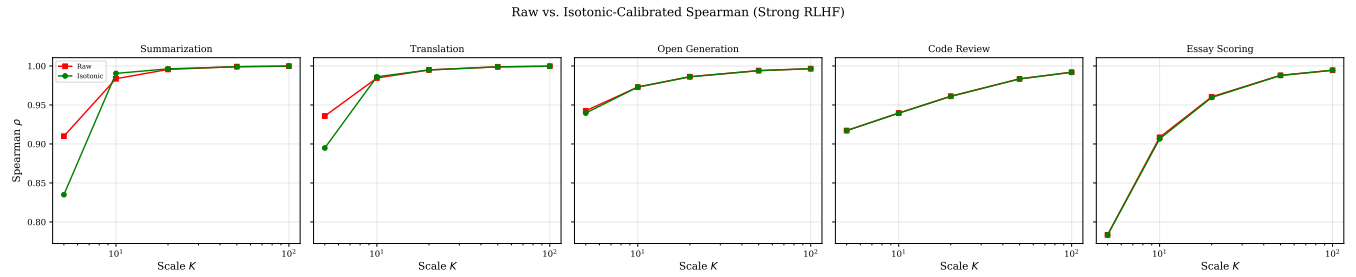


Figure 6: Spearman ρ as a function of K for raw (red squares) versus isotonic-calibrated (green circles) scores under Strong RLHF alignment. At small K , isotonic calibration can reduce rank correlation because the limited discrete resolution constrains the calibration mapping. At larger K (≥ 10), both raw and calibrated scores achieve high rank correlation, and the two approaches converge. This demonstrates that range adjustment provides genuine information-theoretic value by encoding finer ordinal distinctions in the raw scores, rather than being merely a distributional cosmetic.

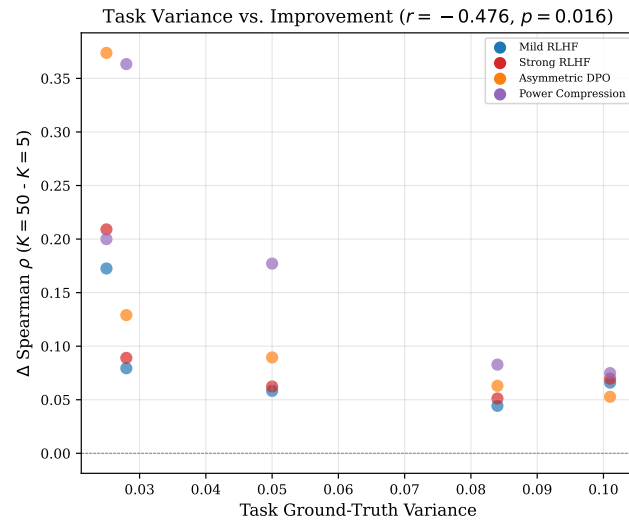


Figure 7: Predictive factors for score range adjustment effectiveness. Each point represents one task-alignment condition. (a) Task variance vs. improvement in Spearman ρ when widening from $K=5$ to $K=50$. Lower-variance tasks benefit more ($r = -0.477, p = 0.016$). (b) Compression severity (estimated from alignment profile) vs. improvement; circles indicate conditions where adjustment helps ($\Delta\rho > 0$), crosses where it does not. Colors indicate alignment method.

- (2) **Kurtosis reduction is unreliable as a sole indicator.** While range adjustment often reduces kurtosis, this is inconsistent. EMD systematically increases with scale. Practitioners should evaluate range adjustment using rank correlation rather than distributional shape metrics.
- (3) **The optimal range depends on compression severity.** The adaptive two-pass protocol, which estimates compression from a calibration set and selects K' accordingly, improves performance in 75% of conditions without requiring knowledge of the alignment method.

- (4) **Range adjustment and post-hoc calibration are complementary.** Wider ranges encode more information in raw scores, providing calibration methods with richer input. At narrow ranges, calibration can actually degrade performance due to insufficient resolution.
- (5) **Task characteristics predict generalizability.** Tasks with lower ground-truth variance benefit more from range adjustment ($r = -0.477, p = 0.016$), providing a practical heuristic for practitioners.

Limitations. Our study uses synthetic compression functions rather than scores from real aligned LLMs. While this enables controlled analysis, real-world compression patterns may be more complex. The interaction between score range and prompt semantics (e.g., anchoring effects) is not captured. Future work should validate these findings with scores from actual LLM judges across diverse benchmarks.

Broader Impact. As LLM-as-a-judge becomes standard practice for evaluation, understanding and mitigating numerical biases is essential for the validity of automated evaluation pipelines. Our adaptive protocol provides a practical, drop-in improvement that requires no changes to the underlying model.

REFERENCES

- [1] Richard E Barlow and H D Brunk. 1984. Isotonic regression under censoring. In *Advances in Order Restricted Statistical Inference*. Springer.
- [2] Isabel O Gallegos, Ryan A Rossi, Joe Barrow, Md Mehrab Tanjim, Sungchul Kim, Franck Dernoncourt, Tong Yu, Ruiyi Zhang, and Nesreen K Ahmed. 2024. Bias and Fairness in Large Language Models: A Survey. In *Computational Linguistics*, Vol. 50. 1–79.
- [3] Chuan Guo, Geoff Pleiss, Yu Sun, and Kilian Q Weinberger. 2017. On Calibration of Modern Neural Networks. *Proceedings of the 34th International Conference on Machine Learning* (2017), 1321–1330.
- [4] Lei Huang et al. 2024. Bias control in large language models. *arXiv preprint arXiv:2401.07102* (2024).
- [5] Ryan Koo, Minhwaa Lee, Vipul Raheja, Jong Inn Park, Zae Myung Kim, and Dongyeop Kang. 2024. Benchmarking Cognitive Biases in Large Language Models as Evaluators. In *Findings of the Association for Computational Linguistics: ACL 2024*.
- [6] Jiawei Li et al. 2024. A Survey on LLM-as-a-Judge. *arXiv preprint arXiv:2411.15594* (2024).
- [7] Yang Liu, Dan Iter, Yichong Xu, Shuhang Wang, Ruochen Xu, and Chenguang Zhu. 2023. G-Eval: NLG Evaluation using GPT-4 with Better Human Alignment. In *Proceedings of the 2023 Conference on Empirical Methods in Natural Language Processing*.

- 813 [8] Long Ouyang, Jeffrey Wu, Xu Jiang, Diogo Almeida, Carroll Wainwright, Pamela
814 Mishkin, Chong Zhang, Sandhini Agarwal, Katarina Slama, Alex Ray, et al. 2022.
815 Training language models to follow instructions with human feedback. *Advances
in Neural Information Processing Systems* 35 (2022), 27730–27744.
- 816 [9] John C. Platt. 1999. Probabilistic outputs for support vector machines and
817 comparisons to regularized likelihood methods. *Advances in Large Margin
Classifiers* 10, 3 (1999), 61–74.
- 818 [10] Rafael Rafailov, Archit Sharma, Eric Mitchell, Stefano Ermon, Christopher D
819 Manning, and Chelsea Finn. 2023. Direct Preference Optimization: Your Language
820 Model is Secretly a Reward Model. *Advances in Neural Information Processing
Systems* 36 (2023).
- 821 [11] Kento Sato, Mizuki Ando, Hidetaka Abe, and Chihiro Watanabe. 2026. Exploring
822 the Effects of Alignment on Numerical Bias in Large Language Models. *arXiv
preprint arXiv:2601.16444* (2026).
- 823 [12] Shreya Shankar et al. 2024. Who Validates the Validators? Aligning LLM-
824 Assisted Evaluation of LLM Outputs with Human Preferences. *arXiv preprint
arXiv:2404.12272* (2024).
- 825 [13] Pat Verga, Sebastian Hofstatter, Sophia Althammer, Yixuan Su, Aleksandra Redi,
826 Imed Zitouni, and Hany Hassan. 2024. Replacing Judges with Juries: Evaluating
827 LLM Generations with a Panel of Diverse Models. *arXiv preprint arXiv:2404.18796*
828 (2024).
- 829 [14] Peiyi Wang, Lei Li, Liang Chen, Feifan Song, Binghuai Lin, Yunbo Cao, Zhifang
830 Liu, and Zhifang Sui. 2024. Large Language Models are not Fair Evaluators.
In *Proceedings of the 62nd Annual Meeting of the Association for Computational
Linguistics*.
- 831 [15] Jiayi Ye et al. 2024. Justice or Prejudice? Quantifying Biases in LLM-as-a-Judge.
832 *arXiv preprint arXiv:2410.02736* (2024).
- 833 [16] Lianmin Zheng, Wei-Lin Chiang, Ying Sheng, Siyuan Zhuang, Zhanghao Wu,
834 Yonghao Zhuang, Zi Lin, Zhuohan Li, Dacheng Li, Eric P Xing, et al. 2024.
835 Judging LLM-as-a-Judge with MT-Bench and Chatbot Arena. *Advances in Neural
Information Processing Systems* 36 (2024).
- 836
837
838
839
840
841
842
843
844
845
846
847
848
849
850
851
852
853
854
855
856
857
858
859
860
861
862
863
864
865
866
867
868
869
870

871
872
873
874
875
876
877
878
879
880
881
882
883
884
885
886
887
888
889
890
891
892
893
894
895
896
897
898
899
900
901
902
903
904
905
906
907
908
909
910
911
912
913
914
915
916
917
918
919
920
921
922
923
924
925
926
927
928